MANSOURA JOURNAL OF CHEMISTRY
Official Journal of Faculty of Science, Mansoura University, Egypt
E-mail: scimag@mans.edu.eg ISSN: 2974-4938

Sulfated Zirconia Nanocatalyst Modified by Cerium Oxide

Mai El-Sayad, Sohair A. El Hakam, Shady M. El-Dafrawy and Shawky M. Hassan*

Chemistry Department, Faculty of Science, Mansoura University, Egypt
** Correspondence to: (SM Hassan; email: shawkihassan@gmail.com & smhassan@mans.edu.eg*

Received: 6/ 12/ 2021
Accepted: 19/ 2/ 2022

Abstract: Sulfated zirconia (SZ) and a solid super acid catalyst cerium-supported SZ (Ce/SZ) were prepared using the sol–gel method in an acidic medium. The prepared catalyst was modified through the addition of different amounts of cerous chloride heptahydrate. Scanning electron microscopy, transmission electron microscopy, and X-ray diffraction were used to detect the physiochemical properties of the prepared catalysts. The strength and number of acid sites were detected by potentiometric titration and Fourier transform infrared spectroscopy of the pyridine adsorbed on the catalysts. The catalytic activity of the prepared catalysts was examined by coumarin synthesis. The reaction was conducted by consuming resorcinol and ethyl acetoacetate in the molar ratio of 1:2. In addition, the activity of the prepared catalysts was examined by Fe removal, and a 3, 4-dihydropyrimdone reaction which was performed by consuming urea, benzaldehyde, and ethyl acetoacetate in the molar ratio of 1.5:1:1.

Keywords: Sulfated zirconia, Sol–gel method, Coumarin synthesis, Catalytic activity

1. Introduction

Green and environmental chemistry have attracted significant attention worldwide. A decrease in the discharge of pollutants into the atmosphere is urgently required. Therefore, continuous efforts have been focused on the search for alternatives in chemical processes and the implementation of chemical technologies **(1)**.

Studies on zirconia have been increasingly recognized because of its strong active sites, which are produced through the modification of zirconia when treated with H_2SO_4. This catalyst plays a remarkable role in the synthesis of chemicals, such as coumarin, organic esters, and N, N′-diphenylene diamines. **(2-4).**

Attention has been focused on super acid solids, such as sulfated zirconia (SZ) because of its high number of acid sites, compared to those of other sulfated metal oxides **(5)**. The addition of CeO_2 to ZrO_2–SO_4^{-2} was investigated in this study.

CeO_2 has been used for several years as one of the most important components of automobile catalytic converters. Currently, it is being studied as a mixed oxide in the form of CeO_2. ZrO_2 used in catalytic convertor applications **(6)**.

The sol–gel template method is widely used because it offers idiosyncratic advantages, including high purity, homogenous multi-component, and easy chemical doping of prepared materials. After a while, this method requires thorough hydrolysis of a solution to obtain a colloidal particle (Sol), after which a gel is formed.

This study aimed to determine the extent of improvement, which occurred by the addition of Ce to SZ. This improvement has been detected in many reactions, such as the formation of 7-hydroxy-4-methyl coumarin and 3, 4-dihydropyrimidinone and the removal of heavy metals (Fe) from water. In addition, the relationship between the acidity and catalytic activity was investigated.

2. Experimental process

Zirconium oxychloride ($ZrOCl_2{\cdot}8H_2O$), cerous chloride heptahydrate ($CeCl_3{\cdot}7H_2O$), 100% absolute alcohol (EtOH), 2N sulfuric acid (H_2SO_4), resorcinol ($C_6H_6O_2$), and ethyl acetoacetate (EAA, $C_6H_{10}O_3$) were obtained and used in the experiment.

2.1. Synthesis of catalyst

2.1.1. Preparation of SZ catalyst using the sol–gel method

First, 26.15 g of $ZrOCl_2 \cdot 8H_2O$ was dissolved in absolute ethyl alcohol (EtOH) by putting it on a stirrer for 2–3 h to ensure complete dissolution. Thereafter, 2N sulfuric acid was added dropwise to the zirconia solution at room temperature with continuous stirring. The solvent was transformed into a white gel. Afterward, the gel was dried using a rotary dryer at 90°C.

2.1.2. Synthesis of Ce/SZ Catalyst

Subsequently, 0.02, 0.05, 0.1, and 0.2 Ce/SZ were synthesized by dissolving appropriate amounts of cerous chloride in absolute alcohol (10 mL), followed by stirring for 15 min. After dissolution, they were slowly added to the Zr (gel) sample with stirring at room temperature and dried using a rotary dryer at 90°C. Finally, Ce/SZ was obtained by calcining at 600°C for 3 h at a heating rate of 20°C min^{-1}.

2.2. X-ray

Powder diffraction patterns in the presence of Ni clarified using Cu Kα radiation (λ = 1.540 *Å*) at 40 kV, 30 mA, and a scanning range of 2θ = 18–80. The tetragonal phase of zirconia percentage was determined using the following equation.

$$\%\,Tetragonal = \left[\frac{IT\,(2\theta = 30.15)}{IT(2\theta=30.15)+\left(\frac{IM(2\theta=28.16)+IM(2\theta=31.44)}{2}\right)}\right] x\,100$$

The crystallite size (nm) was determined using the tetragonal zirconia reflection phase after 2 h of 2θ = 30.15°, using the Scherrer equation (7,8, 9,10) as follows:

$$D = \frac{K\lambda}{\beta \cos \theta}$$

where K is the crystallite shape constant (≈1), λ is the radiation wavelength (*Å*), β is the line breadth (radians), and θ is the Bragg angle.

2.3. Transmission electron microscopy (TEM)

Images and particle sizes were observed by TEM using a JEOL JEM-2100 transmission electron microscope operating at 120 kV. The samples were prepared by depositing a suspension of the fine sample powder onto a copper grid coated with a holey carbon foil and dried at ambient temperature.

2.4. Scanning electron microscopy (SEM)

The surfaces of the nanocatalyst samples were observed by SEM (JEOL JSM-6510 LV). The chemical and morphology composition of the examined samples were studied by SEM. The samples were prepared by placing a minute quantity of the catalyst particles on a gold-coated grid prior to the SEM **(11).**

2.5. Brunauer–Emmett–Teller (BET)

The specific surface areas of the samples that were calcined at 600°C were determined by nitrogen adsorption at 196°C within a high-vacuum conventional volumetric glass system. The investigated samples were degassed at 25°C for 3 h under a reduced pressure of 10^{-5} Torr.

2.6. Surface acidity measurements

2.6.1. Nonaqueous Potentiometric Titration

Nonaqueous potentiometric titration was performed to determine the total number of acid sites. After the activation of the catalyst (0.1 g) suspension in acetonitrile (10 mL), the sample was titrated with 0.01N n-butylamine in acetonitrile. The electrode potential for the prepared samples was measured with an Orion 420 digital model using a double junction electrode.

2.6.2. Pyridine Adsorption

The Lewis and Brønsted acid sites for the investigated solid samples were observed by placing investigated samples in a beaker comprising pyridine for one week in a high-vacuum oven. Fourier transform infrared (FT-IR) spectrometry was performed on the prepared samples as follows: 0.1 g of KBr was mixed with 0.05 g of the prepared sample in self-supporting discs with a diameter of 30 mm.

3. Catalytic activity

3.1. Coumarin reaction

The activity of the prepared catalyst samples was investigated via a Pechmann condensation reaction, which was performed under reflux conditions. A mix of EAA and resorcinol was refluxed with the freshly calcined catalyst.

The molar ratio of the resorcinol and EAA mix was 1:2 in a round flask. It was refluxed in

an oil bath for 2 h at 120°C in the presence of 0.1 g of the freshly activated catalyst. Pechmann reaction of resorcinol (1) with ethyl acetoacetate (2) to produce 7-hydroxy-4-methylcoumarin (3).

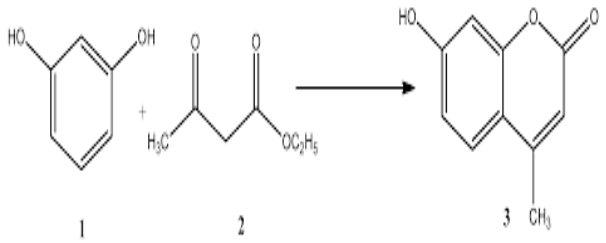

The resultant sample was poured into a beaker (50 mL) containing crushed ice and followed by scratching until the solid product was formed. These conditions were selected based on previous studies **(12, 13)**. The product was detected by melting point (185°C) and FT-IR analysis. The yield percentage of the 7-hydroxy-4-methyl coumarin was calculated as follows **(14,15)**:

$$\text{Yield (wt. \%)} = \frac{\text{experimental wt. of the product}}{\text{theoretical wt. of the product}} \text{x100}$$

Filtration was used to separate the solid product. The organic compound was dried and extracted with hot ethanol. The undissolved catalyst remained and was separated by filtration from the alcoholic solution. The revocation of the 7-hydroxy-4-methyl coumarin was conducted by solvent evaporation in a hot water bath.

3.2. Synthesis of 3,4-dihydropyrimidinone (Biginelli reaction)

Biginelli reaction (3,4-dihydropyrimdinone) had a long reaction time (20–30h) and the resultant product was in low yield. Recently, Lewis acid has been found to catalyze this reaction. This has been reported in many studies on $ZrCl_4$, $ZrOCl_2$, $FeCl_3$, $CeCl_3 \cdot 7H_2O$, and zeolites **(13-15)**. However, these methods resulted in low and moderate yields of 3,4-dihydropyrimidinone **(16,17)**. To solve these problems, the 3,4-dihydropyrimidinone was prepared at 80 ^oC using, (benzaldehyde: EAA: urea) in ethanol with a molar ratio of 1:1:1.5 in the presence of 0.05 g of the Ce/SZ nano-catalyst. The progress of the reaction was determined by thin-layer chromatography. After the reaction filtration, the Ce/SZ nano-catalyst was washed and dried (**18**). In addition, the combined organic layers were washed and dried, and the solvent was evaporated under reduced pressure. Afterward, the pure product was obtained without further purification.

3.3. Removal of Heavy Metal (Fe) from water

The elimination of heavy metals such as free Fe ions from an aqueous solution has been investigated by electrolytic precipitation, deposition with alkali hydroxide, lime, ion exchange, and reverse osmosis. Although these methods are known and widely used, there are certain drawbacks in their results. These drawbacks include imperfect metal elimination, exclusion of secondary waste, and metal-demeanor sludge or wastes. A new method, adsorption, offers excellent results in the exclusion of Fe ions; it is inexpensive and effective **(19, 20)**. The preparation of a solution (100 mg L^{-1}) of Fe(III) stock was performed using $FeCl_3 \cdot 6H_2O$. The percentage of the metal ions recovery (Recovery %) was determined.

$$\textbf{Recovery \%} = \frac{(\mathbf{C_o - C_o})}{\mathbf{C_o}} \textbf{ x 100}$$

where C_o is the initial concentration (mg L^{-1}) and C_e is the residual concentration (mg L^{-1}) of the metal ions. The removal of Fe from water was investigated using samples with different metal (C_e) contents loaded on SZ.

4. Results

4.1 X-ray diffraction (XRD):

The effect of different Ce amounts on the crystallite size of SZ and crystal phases observing (XRD) patterns shown in Fig. (1). A monoclinic phase was indicated at the peaks where (2θ=28° & 31°). However, the tetragonal phase, which was the most catalytically active, was noticed at a peak where 2θ = 30°.

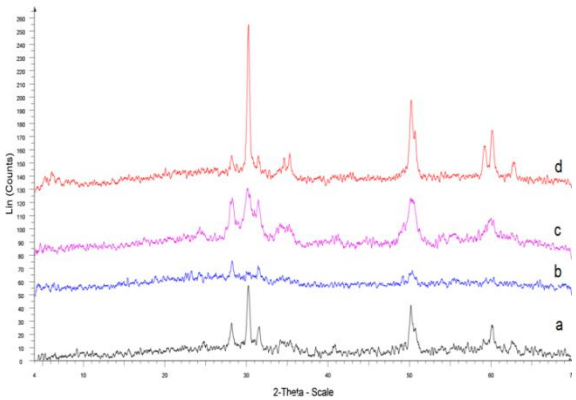

Fig (1): (a) parent Ce/SZ , (b) 0.02 Ce/SZ ,(c) 0.05 Ce/SZ and (d)0.1Ce/SZ calcinedat 600 °C

It was observed that the undoped parent SZ exhibited a major tetragonal phase and a monoclinic phase. The SZ with the 0.02 Ce showed a transformation of the tetragonal phase to a monoclinic phase, which was major in the 0.02 Ce/SZ. The 0.05 Ce/SZ showed more stable tetragonal phases than monoclinic phases. Additionally, the 0.1 Ce/SZ showed the most stable tetragonal phase as shown in Fig (2). The smaller the particle sizes the greater the surface energy contributing to the mono-clinic phase stability on the surface (sulfate group) or in the bulk (cationic dopant).

4.2. TEM

The TEM images reveal the variation in particle size of the Ce/SZ with different Ce contents calcined at 600°C (Fig 3). The Ce content affected the particle size. The particle size of the SZ parent decreased when the Ce content was increased up to 0.2, which led to large particles. These results correspond with those of the XRD analysis.

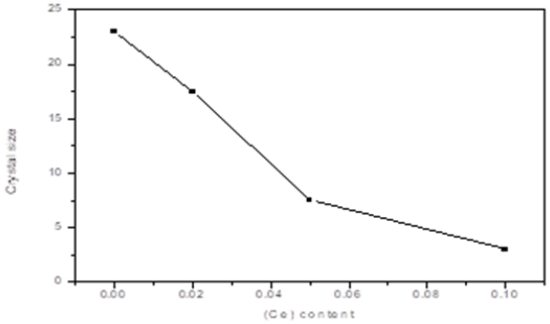

Fig. (2): Effect of different CeO_2% on crystal size

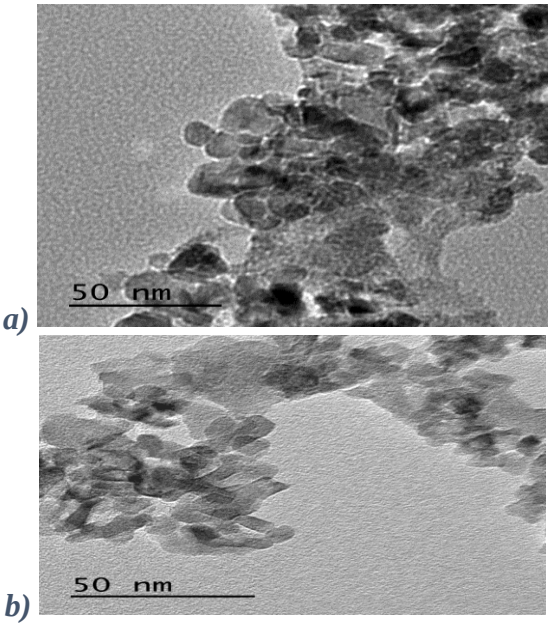

a)

b)

Fig (3): TEM Images of Ce/SZ with (a) 0.02 Ce/SZ and (b) 0.1Ce/SZ calcined at 600^{o}C

4.3. SEM

The surface structure of the SZ with different Ce contents at a calcination temperature of 600°C is shown in the SEM images. The 0.1 Ce/SZ catalyst showed better homogeneity than the SZ parent as shown in Fig (4). The results showed a growth in the particle size with agglomerations. This behavior may be due to supersaturation effects, whereas the surface loaded with Ce particles. Increasing Ce contents resulted in particle adhesion and aggregate consolidation by particle growth. Therefore, the supersaturation promoted aggregation by generating large particles.

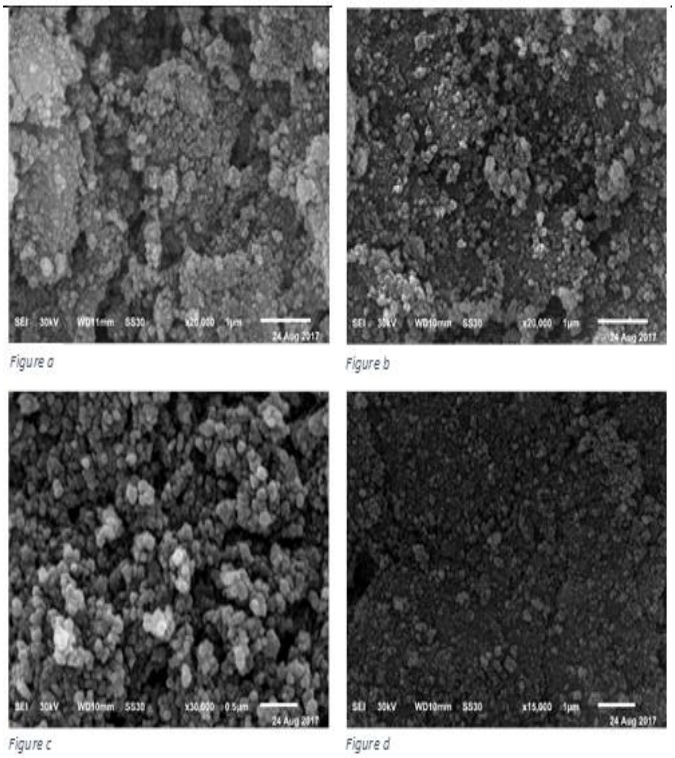

Fig (4): SEM of different CeO2% (a) 0.02 Ce/SZ, (b) 0.05 Ce/SZ (c) 0.1 Ce/SZ (d) parent SZ

4.4. Surface area measurement

The BET analysis of the investigated samples showed type II isotherms with type H_3 or H_4 hysteresis loops, which are characteristic of slit-shaped pores, according to the IUPAC classification. The morphology relates to the surface area of the samples. The results showed that the surface area increased with an increase in the Ce content up to 0.1 and finally decreased, Fig. (5), this can be attributed to the increase in sulfated concentration blocking the active sites on the surface.

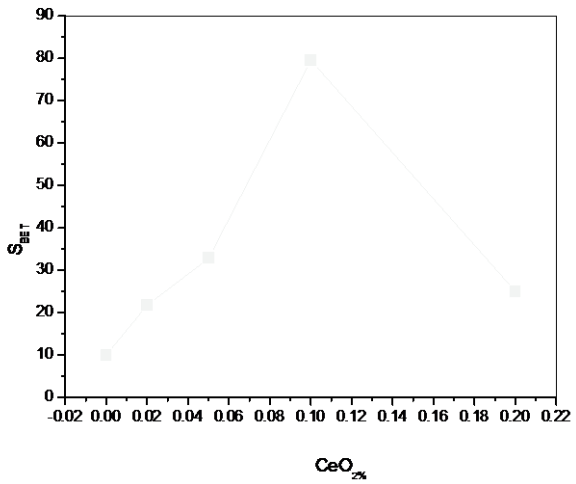

Fig. (5) Variation of $S._{BET}$ with CeO_2 content

4.5. Surface acidity measurements

4.5.1. Nonaqueous Titration

The characteristics of surface acidity, which include the total number of acid sites and acidic strength, were investigated by nonaqueous titration using n-butyl amine p^{ka} = 10.73. In this technique, the total number of acid sites is indicated by the range where the plateau is reached, while the initial electrode potential (E_i) indicates the acid strength of the surface sites. In addition, there is a relationship between the electrode potential and surface acidity of the catalyst, as shown in Table (1). The total acidity of the Ce/SZ catalysts calcined at 600°C increased with an increase of Ce content. It reached its maximum at 0.1 g of Ce. As the percentage of coverage of the Ce on the SZ surface directly increased, the percentage and strength of the acid sites increased. The prepared sample that contains cerium amount more than 0.1 gm. shows a decrease in acidity and the acid strength. This probably due to agglomeration of Ce on the surface.

4.5.2. Pyridine adsorption

The Brønsted and Lewis acid sites were investigated by the adsorption of pyridine as a base on the surface of the catalysts The FT-IR pyridine adsorption spectra showed the region within 1100–1700 cm^{-1} of the Ce/SZ catalyst calcined at 600°. All the samples showed typical bands of adsorbed pyridine at approximately 1449 and 1600 cm^{-1} on the Lewis acid sites and 1535 and 1632 cm^{-1} on the Brønsted acid sites. The band at 1492 cm^{-1} indicated the formation of the adjacent Lewis and Brønsted acid sites.

Table 1: Effect of Ce content on the acidic and catalytic properties of Ce/SZ calcined at 600 ^oC

Ce/SZ	E_i (mv)	Total no. of acid x 10^{-20}	B/L	Coumarin yield
0.00	368	0.5578	0.4720	17.5
0.02g	347.9	0.72	0.4877	18.07
0.05 g	382.7	1.1031	0.4665	18.15
0.1 g	350.7	1.2270	0.4944	50.22
0.2 g	313.2	0.3148	0.4746	14.218

The percentage of Lewis–Brønsted acid sites can be calculated using the integrated areas or relative intensity of the characteristic bands of pyridine adsorbed on the Lewis and/or Brønsted acid sites. Here, the percentage of the Lewis and Brønsted acid sites was calculated using this equation.

$$\%\ Lewis = \frac{A_L}{A_B + A_L} x100$$

where A_B is the integrated area of the peaks at 1535 and 1632 cm^{-1}, which were attributed to the pyridinium cation adsorbed on the Brønsted acid site. A_L is the intensity at 1444 or 1606 cm^{-1} of the pyridine molecule coordinated to the Lewis acid site. The results are shown in Table (1).

4.5.2. Coumarin reaction

The Pechmann condensation reaction was carried between resorcinol and EAA to yield coumarin using SZ with different Ce contents. The maximum coumarin yield was observed with the 0.1 Ce/SZ catalyst. The coumarin yield decreased with the increase of Ce content above 0.1. Thus, we can conclude concluded that the 0.1 Ce/SZ is the optimum catalysts for the Pechmann condensation of EAA and resorcinol to the 7-hydroxy-4-methyl coumarin.

The activated group played an effective role in the coumarin yield, and the position of the activated group in the phenol ring was due to resonance and its effect on the activation of the aromatic ring **(21,22).**

The catalytic activity depends on two factors: the phenolic substrate activity and the structure of the catalyst used. The reactivity of phenol differed according to the type of catalyst used. The yield obtained from coumarin using phenol over the solid acid catalyst was 65%, while that obtained over SZ was zero **(23-25)**. However, 50% coumarin was obtained over the 0.1 Ce/SZ. This occurred because the substrate was resorcinol, a highly activated phenol with a hydroxyl group at the meta position.

There are two possible mechanisms for the Pechmann condensation reaction used to synthesize 7-hydroxy-4-methyl coumarin (24). The first mechanism depends on proton transfer to the keto group of EAA from the acid sites of the catalyst by the interaction between the EAA and catalyst. The intermediate and ethanol are subsequently produced, owing to the nucleophilic attack by the hydroxyl group of the resorcinol. The intermediate rapidly undergoes cyclization through intermolecular condensation to yield the 7-hydroxy-4-methyl coumarin.

The second mechanism depends on the electrophilic reaction of the chemisorbed EAA on resorcinol, in which chromone is yielded as a side product (3,4 and 7). The applied mechanism in this study is the first mechanism illustrated in scheme (1). This was because there was no chromone obtained over any of the investigated catalysts.

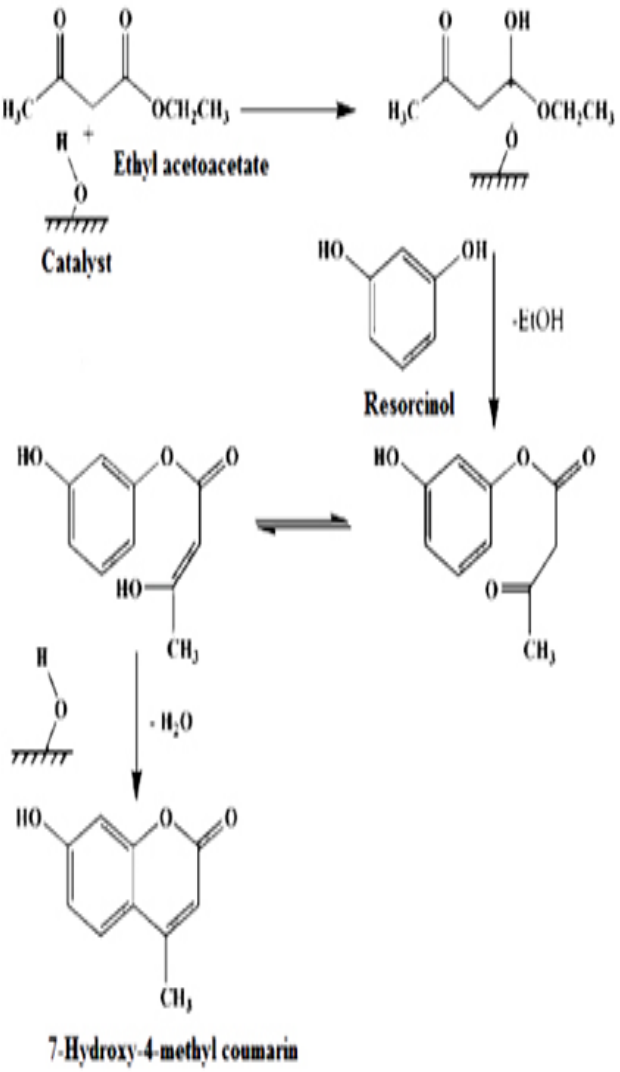

Scheme (1): Mechanism for the Pechmann condensation reaction.

4.5.2.1. Effect of molar ratio on coumarin reaction:

The Pechmann condensation reaction of resorcinol and EAA for the synthesis of 7-hydroxy-4-methyl coumarin occurred at 120°C for 2 h in the presence of 0.1 g of the Ce/SZ calcined at 600°C, using different ratios of the substrate (resorcinol: EAA). It was observed that by increasing the molar ratio of resorcinol: EAA from 1:1 to 1:2, the percentage yield increased from 25 to 50% with 100% selectivity as shown in Fig. (6).

A further increase in the molar ratio to 1:3 decreased the percentage yield to 40%. Therefore, the molar 1:2 was observed to be the optimal ratio for the solvent-free synthesis of 7-hydroxy-4-methyl coumarin. The decrease in catalytic activity may be explained by the increase in the EAA concentration hindering the reaction by blocking the active sites on the catalyst surface.

4.5.2.2. Effect of the weight of Ce on catalytic activity

Table (1) and Fig. (6) show that the percentage yield of 7-hydroxy-4-methyl coumarin gradually increased with an increase in the amount of Ce loaded on SZ until it reached its maximum at 0.1. These results showed that the catalytic activity and Brønsted to Lewis acid sites ratio increased with an increase in the amount of Ce loaded on the samples till 0.1 and decreased with a further increase in the Ce loaded over the sample.

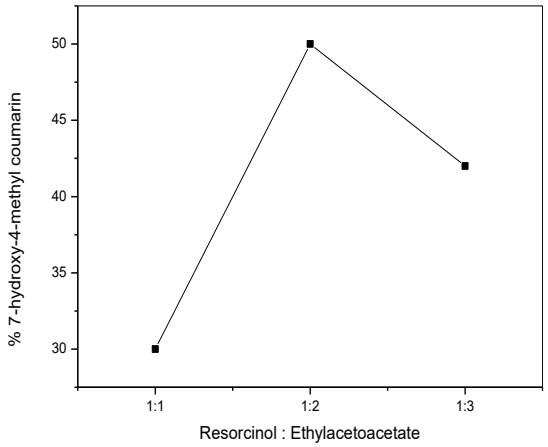

Fig (6): The Effect of molar ratio on the yield % 7-hydroxy-4-methylcoumarin over 0.1 g Ce/SZ

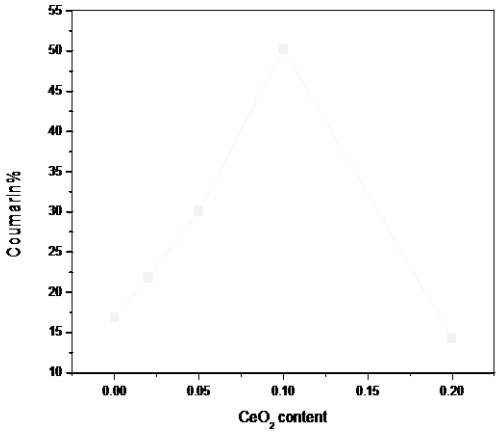

Fig (7): The effect of Ce content on coumarin % at 600 ^{o}C

4.6. Synthesis of 3, 4-dihydropyrimidinone

To increase the percentage yield of the Biginelli reaction (synthesis of 3,4-dihydropyridine), we used Ce/SZ as a catalyst. The 0.1 g Ce/SZ sample showed the highest yield percentage.

4.6.1. Effect of reaction time on the synthesis of 3,4-dihydropyrimidinone

The reaction was performed using 0.05 g of the Ce/SZ nanocatalyst under the same conditions used to investigate the effect of time on the reaction. The results showed that the yield percentage of the product increased with an increase in time from 0.5 to 3 h. The highest yield percentage was observed at 2 h. The 0.1 g sample of Ce/SZ showed the highest yield percentage of 3, 4-dihydropyrimidinone in 2 h = 99%, as shown in Fig (9).

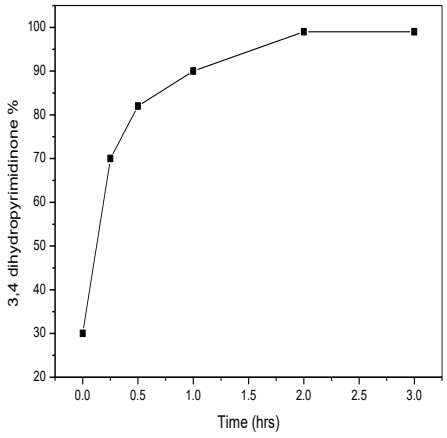

Fig (9): Effect of reaction time on synthesis of 3,4-dihydropyyrimidinone by 0.1 g Ce/SZ catalyst

4.7. Removal of heavy metal (Fe) from water

The results of the experiments with varying amount of Ce loaded on SZ showed an increase in the removal percentage of Fe ions from water. The percentage increased up to a Ce/SZ content of 0.1 and decreased as shown in Fig. (10). This was because the increased availability of active adsorption sites arising from the intension in the effective surface area resulted from an increase in the sorbent dose. Therefore, the 0.1 Ce/SZ is the optimal sorbent for the Fe ions.

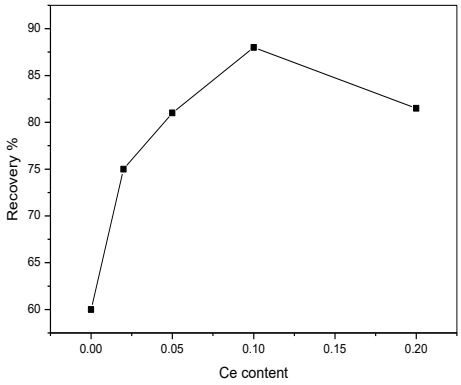

Fig (10): Effect of (Ce) content on recovery percentage of water

5. Conclusion

The sol–gel method was used to prepare Ce-doped SZ. All the prepared samples were calcined at 600°C, and the 0.1 g Ce/SZ sample exhibited the maximum yield of 7-hydroxy-4-methyl coumarin and showed the highest yield in the formation of 3,4-dihydropyrimidinone. In the recovery of water from heavy metals such as Fe ions, the 0.1 g Ce/SZ also showed the highest yield. The XRD analysis of the prepared samples showed that the 0.1 g Ce/SZ sample possessed the maximum tetragonal phase content. These results were confirmed by TEM, which revealed that the SZ particle decreased with an increase in the Ce content up to 0.1. SEM showed that the 0.1 g Ce/SZ sample had more homogeneity than the SZ parent.

References:

1. P. Fornasiero, J. Kaspar, M. Graziani, (1997). *J. Catal.*, 167
2. V.S. Marakatti, G.V Shanbhag, and A.B Halgeri, (2013) *J. Appl. Catal. A: Gen.* **451** 7.

3. A. Sinhamahapatra, N. Sutradhar, S. Pahari, H.C. Bajaj, A.B. Panda, (2011) *J. Appl. Catal. A: Gen.* **394** 93.
4. S. Ghodke, and U. Chudasama, (2013) *J. Appl. Catal. A: Gen.* **453** 219.
5. D. Fraenkel, N.R. Jentzsch, Ch.A. Starr and P.V. Nikrad, (2010) *J. Catal.*, **274** 29.
6. B. Karami, and M. Kiani, (2011).*J. Catal. Comm.*, **14**
7. M.M Heravi, S. Khaghaninejad, and M. Mostofi, (2014) *J. Adv. Hetero. Chem.*, **112** 1.
8. B.M. Devassy, F. Lefebvre, W. Bohringes, J. Fletcher, and S.B. Halligudi, (2005) *J. Mol. Catal A: Chem* **236** 162.
9. A. Patterson, *J. Phys. Rev.*, 56 (1939) 978.
10. R. Jenkins, and R.L. Snyder, (1996) *J. Chem. Anal.*, **138** 335.
11. K. Vos. N. Vandenberghe, and J. Elsen, (2014) *J. Earth Sci. Rev.*, **128** 93.
12. M.S. Wu, P. He and X.Z. Zhang, (2010) *South. Afric. J. chem.*, **63** 224.
13. M.G. Kulkarni, S.W. Chavhan, M.P. Shinde, D.D. Gaikwad, A.S. Borhade, A.P. Dhondge, Y.B. Shaikh, V.B. Ningdale, M.P. Desai and D.R. Birhade, *Belistein*(2009) *J. Org. Chem.*, **5** 1.
14. J.K. Joseph, S.L. Jain, S. Singhal and B. Sain, (2011) *J. Ind. Eng. Chem. Res.*, **50** 11463.
15. F. Mengl, Z. Li, Z. Xu, W. Fang, M. Liu, Y. Wang, J. Zhang, W. Wang, D. Zhao and X. Guo, (2013) *J. Mater. Chem. A.*, **1** 7235.
16. K. Abou-El-Sherbini, P. G-Weidler, D. Schiel, M.H. Amr, H. Niemann, Sh. El-Dafrawy, W.H. Holl, (2014)*J. Green and Subain. Chem.*, 4
17. S. Abd EL-Hakam, Sh.M. El-Dafrawy, S. Fawzy, Sh.M. Hassan, (2012) 1. *J. Intern. J. Sci. Res.*, **3**
18. Sh. M. El-Dafrawy, (2015) *J. Catal. and Catal. Res.*, **1** 5.
19. Sh.M. El. Dafrawy, *Intern. J. Sci. and Res.* 2319
20. Sh.M. El-Dafrawy, H.M. Youssef, W.O. Toamah and M.El Dafrawy, *Egypt.* (2015) *J. Chem*, **6** 579
21. M.S. Abdel-Aziz, Kh.S. Abou-El-Sherbini, E.M.A. Hamzawy, M.H.A. Amr, Sh.M. El-Dafrawy, (2015) *J. Appl. Biochem. Biotechn.*, **176** 2225
22. Sh.M. El-Dafrawy, S.Fawzy, Sh.M. Hassan, (2017) *J. Trends Appl. Sci.* **12** 1
23. Sh.M. El-Dafrawy, M. Farag and Sh.M. Hassan, (2013) *J. Chem. Interm.* 39
24. Sh.M. El-Dafrawy, M. Farag, S. Abd El-Hakam and Sh.M. Hassan, *Egypt*(2017) *J. Chem.*, **60** 329.
25. A.I. Ahmad, Sh.M. El-Dafrawy, F.T. Al-Shorifi, (2017) *Int. J. Nano and Mater. Sci.* 30.